

Cooperativity Between Low-Valent Iron and Potassium Promoters in Dinitrogen Fixation

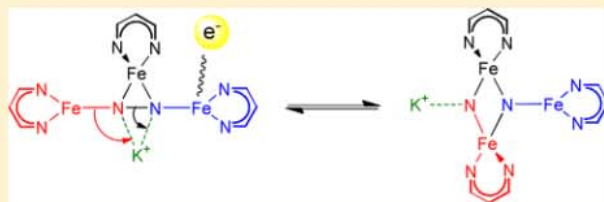
Travis M. Figg, Patrick L. Holland,^{‡,*} and Thomas R. Cundari*

Department of Chemistry and Center for Advanced Scientific Computing and Modeling (CASCaM), University of North Texas, Denton, Texas 76203-5017, United States

[‡]Department of Chemistry, University of Rochester, Rochester, New York 14627, United States

* Supporting Information

ABSTRACT: A density functional theory (DFT) study was performed to understand the role of cooperativity between iron-diketiminato fragments and potassium promoters in N₂ activation. Sequential addition of iron fragments to N₂ reveals that a minimum of three Fe centers interact with N₂ in order to break the triple bond. The potassium promoter stabilizes the N³ ligand formed upon N₂ scission, thus making the activated iron nitride complex more energetically accessible. Reduction of the complex and stabilization of N³ by K⁺ have similar impact on the energetics in the gas phase. However, upon inclusion of continuum THF solvent effects, coordination of K⁺ has a reduced influence upon the overall energetics of dinitrogen fixation; thus, reduction of the trimetallic Fe complex becomes more impactful than coordination of K⁺ vis-a-vis N₂ activation upon the inclusion of solvent effects.



INTRODUCTION

Conversion of dinitrogen (N₂) into useful materials is desired for uses such as the production of ammonia (NH₃), one of the most important chemicals used in synthetic fertilizers.¹ However, N₂ is difficult to activate, because of the inherent strength of the N–N triple bond (235 kcal/mol). The dominant industrial method for the reductive cleavage of N₂ and formation of NH₃ is the catalytic reduction of N₂ with dihydrogen (H₂) via the Haber–Bosch process. Because of its low cost, iron is commonly used to catalyze the Haber–Bosch process.² Potassium promoters improve the catalytic activity of iron surfaces, partially because of an increase in the rate constant for N₂ dissociation on the iron surface.³ In synthetic compounds, cooperative binding of N₂ by iron and alkali metal ions has been shown to weaken the N–N bond more than iron alone, and this trend has been extended to chromium,⁴ cobalt,^{5,6} and nickel.⁷ However, these systems do not cleave the N–N bond. Further progress in cooperative N₂ activation requires better understanding of two key factors: (1) the reductive cleavage of the N₂ bond, and (2) the role of promoters such as potassium.

Recently, Holland and co-workers reported a soluble iron-diketiminato ([Fe]) system that can cleave N₂ to give a bis(nitride) intermediate (Figure 1).¹¹ Relatively few Fe-nitride complexes have been reported in the literature that involve more than two Fe centers interacting with nitride atoms, and no others are derived from N₂.^{12,13} The complex in Figure 1 arises from cleavage of N₂, and has three [Fe] fragments interacting directly with nitrides and a fourth [Fe] interacting indirectly through a series of Cl and K interactions. Although this system is not catalytic, the chemistry depicted in Figure 1 is

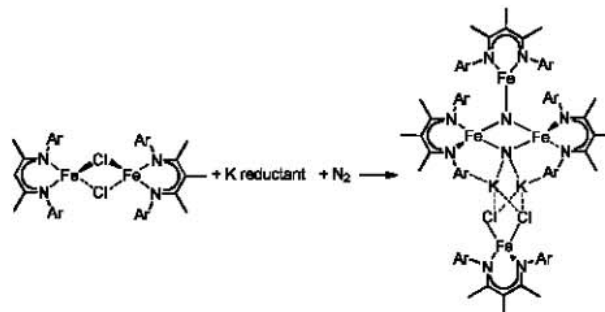


Figure 1. Structure of the soluble iron-diketiminato-nitride complex formed upon cleavage of the N₂ triple bond. Ar = 2,6-C₆H₃Me₂.

a potential stepping stone to a better understanding of catalysts for solution-phase N₂ fixation.

In this study, density functional theory (DFT) calculations are employed to understand the role of cooperativity between multiple iron-diketiminato fragments. For example, how many Fe atoms are needed to cleave the N₂ bond in the reduction step, and what intermediates are potentially involved? Theoretical calculations have greatly aided in understanding N–N bond cleavage.^{8–10} The research reported here indicates that interaction of N₂ with more metal centers increases the N–N activation, and thus N₂ fixation benefits from cooperation between metals. The present calculations also yield insight into the effects of K promoters in N₂ fixation.¹⁴

Received: January 19, 2012

Published: June 26, 2012

COMPUTATIONAL DETAILS

Density functional theory (DFT) was used to facilitate comparison between the various ground states of the $[\text{Fe}]_3\text{N}_2$ and $[\text{Fe}]_3(\text{N})_2$ species. The Gaussian 09 software package¹⁵ was used for geometry optimizations, and frequency calculations. The B3LYP/6-31+G(d) calculated geometries and properties of $[\text{Fe}]\text{N}_2$ and $[\text{Fe}]_2\text{N}_2$ species are similar to those previously reported from multiconfiguration self-consistent field (MCSCF) computations.^{16–18} Additional continuum solvent corrections are computed in tetrahydrofuran (THF), using the SMD formulation, and are compared to the gas-phase energetics.¹⁹ Since computations on the monometallic and bimetallic Fe–diketimate species have been reported previously,^{16–18} the present contribution focuses on trimetallic species, the interactions of K^+ on important intermediates in an array of binding modes, and the role of reduction.

Various isomers of the $[\text{Fe}]_n\text{-N}_2$ complexes were calculated in all plausible spin states. Free energies are quoted, relative to separated starting materials: (iron–diketimate) $_n + \text{N}_2$ (n = number of $[\text{Fe}]$ fragments involved in the reaction). Bond lengths are given in Ångströms. Initial attempts to model the tetra-iron complex in the Figure 1 molecule with ONIOM techniques revealed that the substituents need to be modeled with full QM techniques, because of the importance of K^+ –arene interactions. The ligands were thus truncated to $\text{C}_3\text{N}_2\text{H}_5$ for computational expediency; in previous reports, we have found that this truncation gives iron–dinitrogen (Fe-N_2) complexes with metrical and spectroscopic parameters that agree well with the experiment and faithfully represents the core electronic properties of larger –diketimate supporting ligands.^{6,16–18} The studies here are limited to a single K^+ ion and three Fe atoms, because the fourth Fe atom in the complex reported by Holland et al.¹¹ interacts indirectly with the Fe_3N_2 core via K^+ –arene interactions.

RESULTS AND DISCUSSION

This paper explores the effect of sequentially adding Fe–diketimate fragments to free N_2 in various binding modes. The experimental route to the complex in Figure 1 starts from potassium reduction of an iron(II)–diketimate starting material to give a presumed iron(I) species that were modeled here as the unsaturated fragment iron–diketimate. Previous work revealed that three-coordinate iron(I) gives strong backbonding into the π^* orbitals of N_2 , and binding of a second fragment enhances N_2 bond lengthening.^{16,18} A single $[\text{Fe}]$ binds N_2 in an end-on (E) fashion in a quartet spin state,

$G_{\text{rel}}(^4\text{E-FeN}_2) = 13$ kcal/mol. The lowest energy bimetallic N_2 complex is end-on/end-on (EE) in a septet state, as seen experimentally for closely related compounds,¹⁸ with $G_{\text{rel}}(^7\text{EE-Fe}_2\text{N}_2) = 40$ kcal/mol. Binding of the second fragment is thus cooperative (defined here as the extra stabilization in a bimetallic complex beyond that expected from two monometallic interactions) by $40 - (2 \times 13) = 14$ kcal/mol. The ligation of a second E-Fe increases the N_2 bond length by 5%, from 1.127 Å to 1.187 Å.

The key advance here is to explore the interaction of more than two iron(I) fragments with N_2 , and so potential binding modes were explored for a third $[\text{Fe}]$ fragment interacting with N_2 . Three isomers of trimetallic complexes were compared: end-on/end-on/side-on (abbreviated EES- Fe_3N_2), end-on/side-on/side-on (abbreviated ESS- Fe_3N_2), and all-side-on (abbreviated SSS- Fe_3N_2). Note that $[\text{S Fe}]$ indicates a side-on interaction of iron with N_2 , which, to our knowledge, has never been observed experimentally in an iron complex; therefore, this study gives insight into the expected geometry of such an interaction. Various conformers within each family were explored; the lowest energy geometries are given in the figures.

The lowest energy neutral trimetallic isomer, Figure 2 (left), is calculated to be $^{10}\text{EES-Fe}_3\text{N}_2$, $G_{\text{rel}} = 62$ kcal/mol, with an

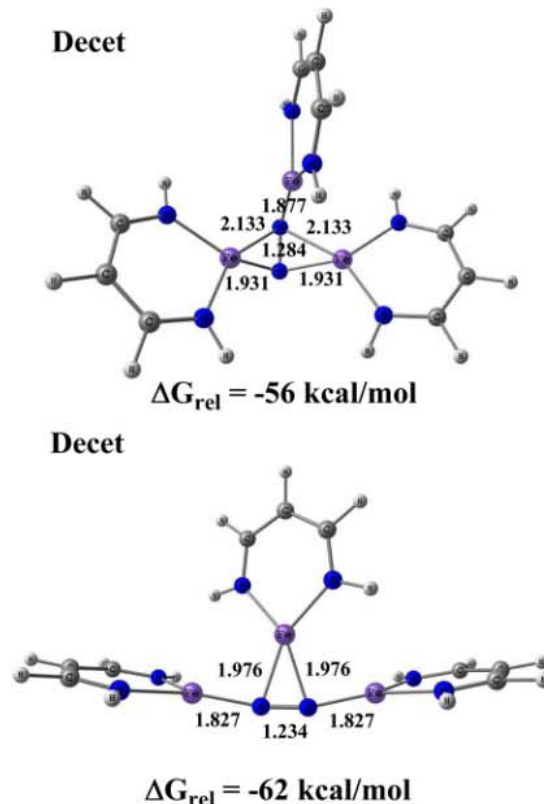


Figure 2. B3LYP geometries of $^{10}\text{EES-Fe}_3\text{N}_2$ (top) and $^{10}\text{ESS-Fe}_3\text{N}_2$ (bottom). The superscript numeral denotes the lowest energy multiplicity ($2S + 1$). Bond lengths given in Å. G_{rel} is calculated relative to isolated $[\text{Fe}]$ and N_2 .

N-N bond length of 1.234 Å. A $^{10}\text{ESS-Fe}_3\text{N}_2$ linkage isomer (Figure 2, right), $d_{\text{NN}} = 1.284$ Å, is only 6 kcal/mol higher than the calculated lowest energy isomer. SSS- Fe_3N_2 isomers were calculated to be thermodynamically unfavorable (by 12 kcal/mol), with respect to those in Figure 2, and, therefore, are not discussed further. Binding of the third $[\text{Fe}]$ fragment to $^7\text{EE-Fe}_2\text{N}_2$ to give $^{10}\text{EES-Fe}_3\text{N}_2$ is found to release 22 kcal/mol, which is 5 kcal/mol less exergonic than the binding of a second $[\text{Fe}]$ fragment to $^4\text{E-FeN}_2$. Importantly, both EES and ESS isomers are energetically accessible, and each lengthens the N-N bond significantly more than two iron fragments in $^7\text{E-Fe}_2\text{N}_2$.

Interestingly, $^6\text{ESS-Fe}_2(\text{N})_2$, which is an isomer with a cleaved N-N bond where $(\text{N})_2$ denotes a bis(nitride) complex, was also present (Figure 3). This complex has a N-N distance of 2.598 Å and a relative G_{rel} of 40 kcal/mol. One of the two nitrides in this species is attached to only two Fe atoms. This nitride nitrogen forms an apparent double bond to one of the Fe atoms, with $d_{\text{FeN}} = 1.654$ Å, which is a relatively strained interaction that may explain why it is 16 kcal/mol less stable than $^{10}\text{ESS-Fe}_3\text{N}_2$ (see Figure 4).

Transformation from $\text{EES-Fe}_3\text{N}_2$ to $\text{ESS-Fe}_3(\text{N})_2$ was explored by scanning the potential energy surfaces of low energy sextet, octet, and decet spin state pathways (Figure 3). The scans reveal low (<5 kcal/mol) barriers for the transformation on each of the three potential-energy surfaces (see Supporting Information). Thus, calculations imply that

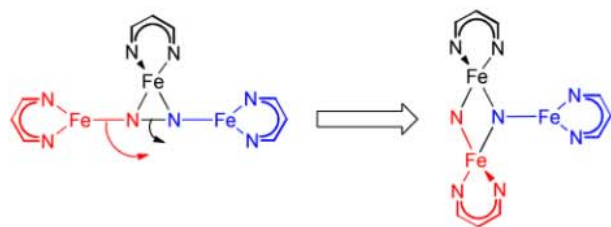


Figure 3. Potential energy scans (red/black arrows) between EES- Fe_3N_2 (left) and ESS- $\text{Fe}_3(\text{N})_2$ (right) indicate small barriers to N_2 scission.

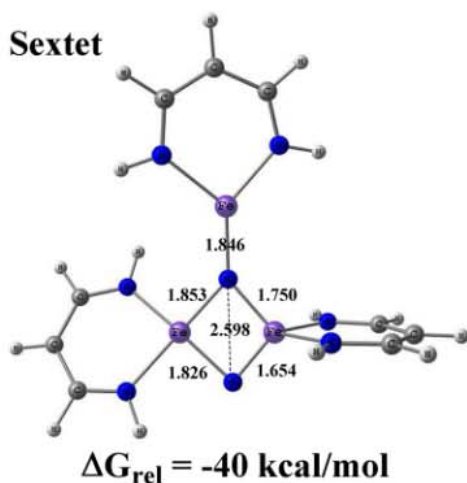


Figure 4. B3LYP calculated geometry of ${}^6\text{ESS-Fe}_3(\text{N})_2$ with a broken N_2 bond. (Bond lengths given in Å.) G_{rel} is calculated relative to isolated $[\text{Fe}]$ and N_2 .

isomerization could be kinetically rapid as a part of the reaction leading to N_2 cleavage, but that the N-N cleavage is thermodynamically unfavorable for the neutral cluster.

Inspection of Figure 1 indicates several K^+ directly interacting with the π -system of the aryl substituents and the nitriles.⁸ Several potential roles of the potassium in the N-N cleavage can be envisioned: K^+ may enforce geometrical constraints, stabilize the nitride (N^3), and/or increase the π -backbonding capacity of the Fe centers, as proposed for the heterogeneous catalyst.¹ To assess the impact of K^+ on N_2 fixation, a K^+ ion was placed in several locations in proximity to the N_2 moiety for the low-energy dinitrogen and dinitride structures (i.e., ${}^{10}\text{EES-Fe}_3\text{N}_2$ with an intact N_2 and ${}^6\text{ESS-Fe}_3(\text{N})_2$ with a broken N_2 bond), respectively. The addition of K^+ to ${}^{10}\text{EES-Fe}_3\text{N}_2$ always rearranges upon DFT geometry optimization to the structure in Figure 5 (left). Binding of K^+ to ${}^{10}\text{EES-Fe}_3\text{N}_2$ is exergonic by 19 kcal/mol and the calculated lowest energy multiplicity of EES- $\text{Fe}_3\text{N}_2\text{K}$ remains a decet. The NN bond is elongated from 1.234 Å to 1.268 Å (3%) upon K^+ addition. The addition of K^+ to ${}^6\text{ESS-Fe}_3(\text{N})_2$ yielded the geometry in Figure 4 (right), with the sextet remaining the lowest energy spin state. The addition of K^+ to ${}^6\text{ESS-Fe}_3(\text{N})_2$ is 11 kcal/mol more exergonic than the K^+ addition to ${}^{10}\text{EES-Fe}_3\text{N}_2$. Thus, the addition of K^+ stabilizes the bis(nitride) product more than the bridged N_2 complex in the gas phase. However, the nitride complex continues to have one unusually short Fe-N bond.

Addition of K^+ to ${}^6\text{ESS-Fe}_3(\text{N})_2$ makes the resulting bis(nitride) (Figure 4) more energetically accessible, relative

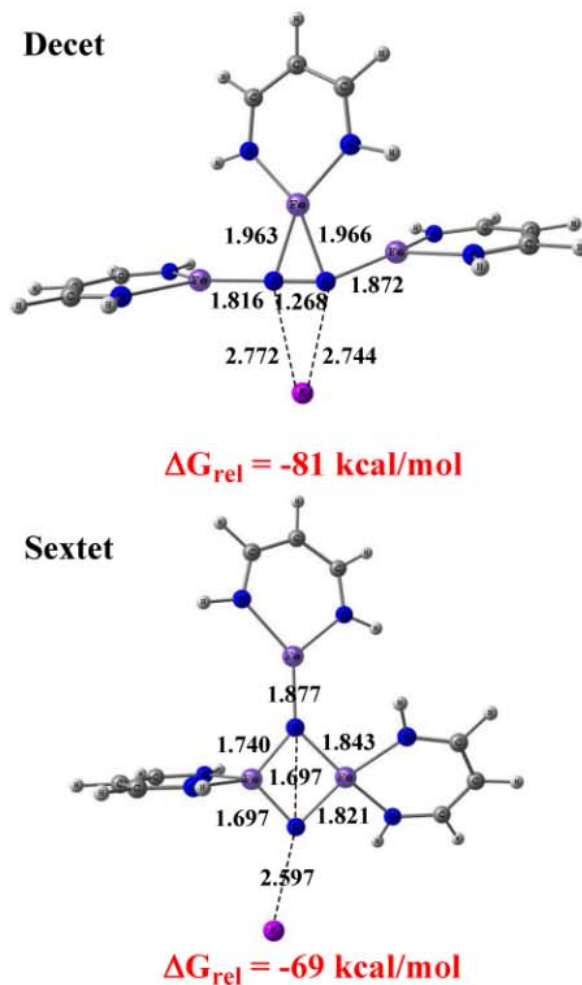


Figure 5. B3LYP structures resulting from the addition of K^+ to ${}^{10}\text{EES-Fe}_3\text{N}_2$ (top) and ${}^6\text{ESS-Fe}_3(\text{N})_2$ (bottom). G_{rel} is calculated relative to isolated $[\text{Fe}]$ and N_2 .

to the dinitrogen isomers, with a free energy for the reaction ${}^6\text{ESS-Fe}_3(\text{N})_2\text{K}^+ \rightarrow {}^{10}\text{EES-Fe}_3\text{N}_2\text{K}^+$ of only 12 kcal/mol, which is roughly half the comparable isomerization free energy in the absence of K^+ . Analysis of calculated atomic charges (see the Supporting Information) suggests that greater stabilization of the N^3 ligand by K^+ coordination is responsible for the diminution of the endergonicity in the nitrogen scission reaction.

Finally, an electron was added to the ${}^{10}\text{EES-Fe}_3\text{N}_2$ complex to mimic reduction by the fourth Fe(1) fragment in the experimental reaction. This yielded $[{}^9\text{EES-Fe}_3\text{N}_2]$ as the lowest energy state, and resulted in only slight geometric distortion (root-mean-square deviation (rmsd) = 0.22 Å). The largest perturbation was the elongation of one Fe-N bond from 1.976 Å to 2.089 Å for the $[\text{S-Fe}]$ fragment, which coincided with an increase of atomic charge on the nitrogen involved in the bond, from 0.19 to 0.58. The added electron occupies a nonbonding, Fe-based orbital, Figure 6, consistent with the minor change in geometry upon reduction. Thus, addition of a single electron to the tri-iron structure has a minor impact on the degree of N_2 activation by trimetallic EES- Fe_3N_2 .

On the other hand, the addition of an electron to ${}^6\text{ESS-Fe}_3(\text{N})_2$ gave a significant effect. Reduction yielded $[{}^5\text{ESS-Fe}_3(\text{N})_2]$ as the lowest energy state. The distance between the

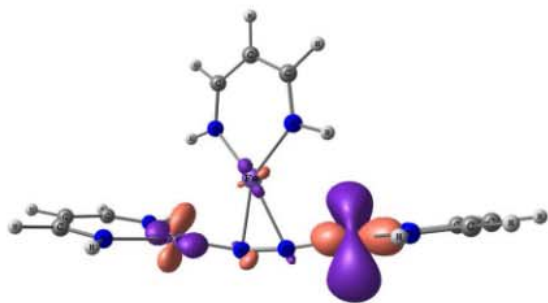


Figure 6. Highest occupied molecular orbital (HOMO) for ${}^9[\text{EES-Fe}_3\text{N}_2]$ complex in which the added electron occupies a nonbonding metal-based orbital.

nitride ligands is shortened from 2.598 Å to 2.587 Å. The added electron was found to occupy a bonding Fe-nitride orbital (Figure 7). A K^+ ion was added to the reduced complexes

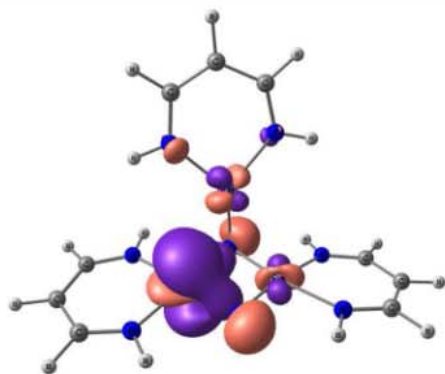


Figure 7. HOMO for ${}^5[\text{ESS-Fe}_3(\text{N})_2]$ in which the added electron occupies a bonding metal-nitride based orbital.

${}^9[\text{EES-Fe}_3\text{N}_2]$ and ${}^5[\text{ESS-Fe}_3(\text{N})_2]$ changing the overall charge on the cluster model to neutral; the resulting complexes were found to possess the same ground spin states as their anionic precursors (Figure 8).

The addition of K^+ to the reduced species makes the ${}^5[\text{ESS-Fe}_3(\text{N})_2\text{K}]$ cluster 3 kcal/mol more stable than ${}^9[\text{EES-Fe}_3\text{N}_2\text{K}]$ (Figure 8). It also gives a structure in which the Fe–N bonds are closer to the experimental crystal structure where the Fe–N bonds proximal to coordinated K^+ are shorter than the corresponding distal Fe–N bond lengths. Therefore, addition of three iron(I) fragments, a K^+ ion, and an electron makes N–N cleavage favorable, presumably because of the stronger interaction of the K^+ cation with the anionic nitride core.

While gas-phase simulations may more appropriately model an industrial nitrogen fixation catalyst, the inclusion of solvent effects is more pertinent to attempt to create a homogeneous version. Continuum solvation corrections in THF were thus computed and compared to the gas-phase energetics to assess the impact of solvation on the reactions of interest. The THF thermodynamics (Figure 9 (right, blue border)) are calculated to be similar to the gas-phase models with one interesting difference. The thermodynamics of ${}^{10}\text{EES-Fe}_3\text{N}_2$ ${}^6\text{ESS-Fe}_3(\text{N})_2$ are changed little by the inclusion of solvent effects ($G_{\text{gas}} = +22.0$ kcal/mol vs $G_{\text{THF}} = +21.5$ kcal/mol; see Figure 9). Similarly, there is a mild solvent influence calculated for the K^+ and K -ligated reactions (e.g., ${}^{10}[\text{EES-Fe}_3\text{N}_2\text{K}]^+$ ${}^6[\text{ESS-Fe}_3(\text{N})_2\text{K}]^+$, $G_{\text{gas}} = +11.3$ kcal/mol, $G_{\text{THF}} = +14.9$

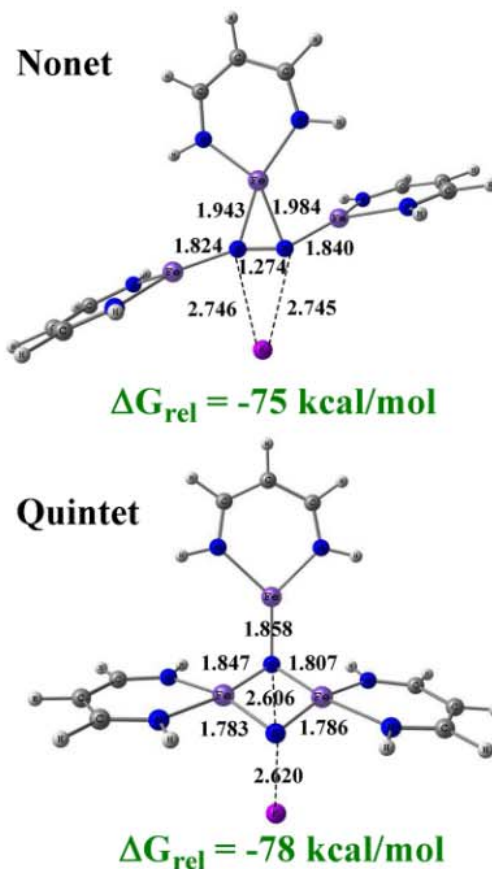


Figure 8. B3LYP structures resulting from addition of K^+ to ${}^9[\text{EES-Fe}_3\text{N}_2]\text{K}$ (top) and ${}^5[\text{ESS-Fe}_3(\text{N})_2]\text{K}$ (bottom). G_{rel} is calculated relative to isolated $[\text{Fe}]$, K^+ , and N_2 .

kcal/mol; see Figure 9). However, reduction upon the nitride-to-bis(nitride) transformation is significantly modulated by solvent, going from endergonic ($G_{\text{gas}} = +8.4$ kcal/mol) to mildly exergonic ($G_{\text{THF}} = -0.5$ kcal/mol) for ${}^9[\text{EES-Fe}_3\text{N}_2]$ ${}^5[\text{ESS-Fe}_3(\text{N})_2]$ (see Figure 9). Comparing the relative G values in gas (G_{gas}) and solvent (G_{THF}) indicates that K^+ becomes less impactful ($G_{\text{gas}}(\text{K}^+) = 10.7$ kcal/mol, $G_{\text{THF}}(\text{K}^+) = 6.6$ kcal/mol) than reduction of the system ($G_{\text{gas}}(\text{e}^-) = 13.6$ kcal/mol, $G_{\text{THF}}(\text{e}^-) = 22.0$ kcal/mol) upon the inclusion of continuum THF solvent effects.

CONCLUSIONS

The present density functional theory (DFT) simulations of the sequential addition of Fe–diketiminato fragments to dinitrogen are important because they show a reasonable series of metal binding and reduction events that cleave N_2 to give a $\text{Fe}_3(\text{N})_2\text{K}$ core like that in a recent experimental report.⁷ In addition to this mechanistic insight, it reveals that three reduced iron centers acting in a cooperative fashion make N_2 cleavage thermodynamically feasible. As summarized in Figure 9, the K^+ promoter stabilizes the nitride ligand of the fixed tri-iron-bis(nitride) isomers by 10 kcal/mol, relative to the N_2 isomers, and N–N cleavage is only favorable when an added electron and potassium are present. However, including a polar continuum solvent reduces the impact of the K^+ on stabilizing the reduced tri-iron-bis(nitride). The results demonstrate that the cleavage of N–N bonds by a reduced iron fragment is greatly influenced by potassium, and also illustrate the impact

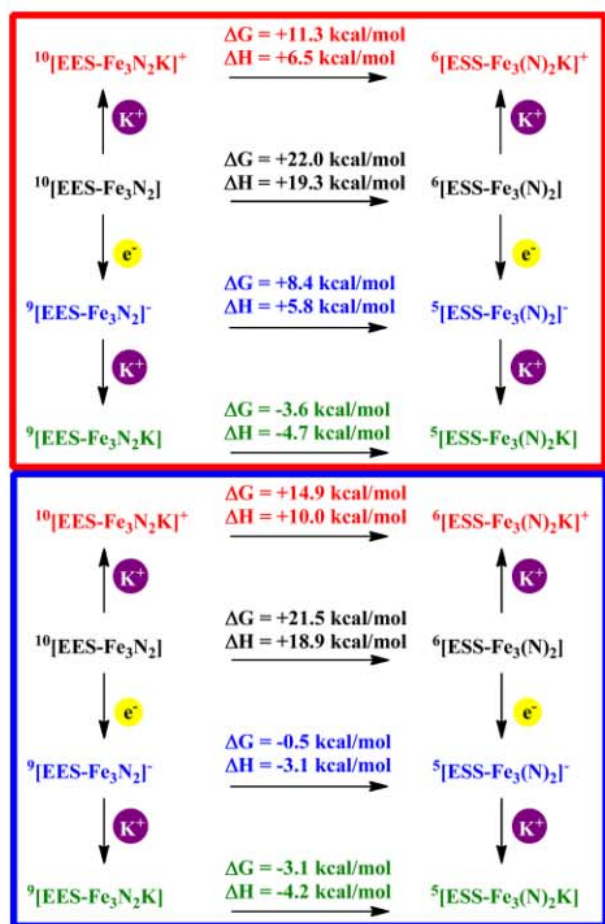


Figure 9. Ladder of calculated gas phase (red border) and solution phase (blue border) relative free energies (G_{rel}) of dinitrogen (left) and bis(nitride) (right) species. Additions of K^+ (red) and electron (blue) to the neutral species (black) are compared (G). Also, the addition of K^+ (green) to the reduced species (blue) is also calculated.

of cooperative Fe binding upon N_2 activation, indicating that at least three iron fragments are needed to cleave N_2 .

ASSOCIATED CONTENT

* Supporting Information

Additional metric data, atomic charges of all calculated species, and full citation for ref 15. This material is available free of charge via the Internet at <http://pubs.acs.org>.

AUTHOR INFORMATION

Corresponding Author

*E-mail: t@unt.edu.

Notes

The authors declare no competing financial interest.

ACKNOWLEDGMENTS

The authors acknowledge financial support from the National Science Foundation (TRC: Nos. CHE-1057785 and CHE-0701247) and the National Institutes of Health (PLH: No. GM065313).

REFERENCES

- Schlogl, R. In *Handbook of Heterogeneous Catalysis*, 2nd Edition; Ertl, G., Knozinger, G., Schuth, F., Weitkamp, J., Eds.; Wiley VCH: Weinheim, Germany, 2008; Vol. 5, pp 2501–2575.
- Mittasch, A. *Geschichte der Ammoniaksynthese*; Verlag Chemie: Weinheim, Germany, 1951.
- Strongin, D. R.; Somorjai, G. *J. Catal.* **1988**, *109*, 51.
- Monillas, W. H.; Yap, G. P.; Theopold, K. H. *Inorg. Chim. Acta* **2011**, *369*, 103.
- Ding, K.; Brennessel, W. W.; Holland, P. L. *J. Am. Chem. Soc.* **2009**, *131*, 10804.
- Ding, K.; Pierpont, A. W.; Brennessel, W. W.; Lukat-Rodgers, G.; Rodgers, K. R.; Cundari, T. R.; Bill, E.; Holland, P. L. *J. Am. Chem. Soc.* **2009**, *131*, 9471.
- Horn, B.; Pfirrmann, S.; Limberg, C.; Herwig, C.; Braun, B.; Mebs, S.; Metzinger, R. *Z. Anorg. Allg. Chem.* **2011**, *637*, 1169.
- Schrock, R. R. *Angew. Chem., Int. Ed.* **2008**, *47*, 5512.
- Khoroshun, D. V.; Musaey, D. G.; Morokuma, K. *Mol. Phys.* **2002**, *100*, 523.
- Cavigliasso, G.; Wilson, L.; McAlpine, S.; Attar, M.; Stranger, R.; Yates, B. F. *Dalton Trans.* **2010**, *39*, 4529.
- Rodriguez, M. M.; Bill, E.; Brennessel, W. W.; Holland, P. L. *Science* **2011**, *334*, 780.
- Bennett, M. V.; Stoian, S.; Bominaar, E. L.; Munck, E.; Holm, R. H. *J. Am. Chem. Soc.* **2006**, *127*, 12378.
- Bennett, M. V.; Holm, R. H. *Angew. Chem., Int. Ed.* **2006**, *45*, 5613.
- Strongin, D. R.; Carrazza, J.; Bare, S. R.; Somorjai, G. A. *J. Catal.* **1987**, *103*, 213.
- Frisch, M. J. et al. *Gaussian 09*, Gaussian, Inc.: Wallingford, CT, 2009.
- Smith, J. M.; Lachicotte, R. J.; Pittard, K. A.; Cundari, T. R.; Lukat-Rodgers, G.; Rodgers, K. R.; Holland, P. L. *J. Am. Chem. Soc.* **2001**, *123*, 9222.
- Pierpont, A. W.; Cundari, T. R. *J. Coord. Chem.* **2011**, *64*, 3123.
- Smith, J. M.; Sadique, A. R.; Cundari, T. R.; Rodgers, K. R.; Lukat-Rodgers, G.; Lachicotte, R. J.; Flaschenriem, C. J.; Vela, J.; Holland, P. L. *J. Am. Chem. Soc.* **2006**, *128*, 756.
- Marenich, A. V.; Cramer, C. J.; Truhlar, D. G. *J. Phys. Chem.* **2009**, *113*, 6378.